

## Radiation Defect Production and Annihilation in KCl near Room Temperature\*

E. SONDER AND L. C. TEMPLETON

*Solid State Division, Oak Ridge National Laboratory, Oak Ridge, Tennessee*

(Received 7 June 1967)

Extended  $\gamma$  irradiation of KCl near room temperature causes the  $F$ -center concentration to saturate between  $10^{18}$  and  $10^{19}$   $\text{cm}^{-3}$ . The saturation concentration is a function of the dose rate and the temperature, and is the same whether approached by production of defects in a fresh sample or by destruction of an excess number of defects in a sample that had been preirradiated under different conditions of temperature or dose rate. The temperature dependence of the saturation level can be described by an empirical activation energy of 0.4 eV between 10 and 50°C. The approach to saturation is approximately 50 times slower than the approach to the aggregation steady state, suggesting that mobile vacancies must travel much further to annihilate than to form  $F$ -aggregate centers. Observations that the approach to saturation cannot be described by simple kinetics and that the shape of decay curves depends upon previous irradiation conditions support the suggestion that the size of the centers with which vacancies annihilate depends upon previous irradiation conditions.

### INTRODUCTION

SIGNIFICANT progress has been made during recent years toward understanding the complex mechanisms involved in radiation defect production in alkali halides. In particular, the discovery by spin resonance of the  $H$  center<sup>1</sup> and other interstitial defects,<sup>2,3</sup> and the analyses of radiation hardening<sup>4,5</sup> and expansion data<sup>6-8</sup> have shown that Frenkel pairs are produced at all temperatures. These results suggest that it is not necessary in most alkali halides to postulate additional mechanisms by which Schottky defects<sup>9</sup> would be produced. Of comparable significance has been the proposal that Frenkel defects can be produced with great efficiency by an excitonic mechanism.<sup>10,11</sup> The production rate predicted by this model is appreciably larger than the measured stable  $F$ -center production rate at temperatures above the liquid-helium range,<sup>12-16</sup> suggesting that secondary reactions, e.g., interstitial-

vacancy recombination and defect aggregation and trapping, occur at the same time that defects are produced. It is such secondary reactions, moreover, which permit accounting for the observed trace impurity<sup>17</sup> variation of color-center production in a fairly straightforward and consistent manner.

Even though the above point of view is not yet universally accepted,<sup>8</sup> it is important to examine the secondary reactions that occur at temperatures above the liquid-helium range. There are three obvious methods by which one might hope to separate the secondary reactions from the primary production process: One can (a) study defect behavior at very short times after pulsed irradiation<sup>18,19</sup>; (b) produce defects at low temperatures where secondary reactions are frozen and then observe the thermally activated processes upon warming<sup>20-25</sup>; and (c) study defect production during lengthy irradiation at temperatures where secondary reactions do take place. From a number of studies on KCl using the first two approaches, we can conclude that interstitial ions and atoms begin to move below 50°K, that self-trapped holes become mobile above  $\sim 150^\circ\text{K}$ , and that negative ion vacancies appear to become mobile above 200°K. The results reported here were obtained by using the third approach of observing the approach to saturation of the color-

\* Research sponsored by the U. S. Atomic Energy commission under contract with Union Carbide Corporation.

<sup>1</sup> W. Känzig and T. O. Woodruff, *Phys. Rev.* **109**, 220 (1958); *J. Phys. Chem. Solids* **9**, 70 (1958).

<sup>2</sup> D. Schoemaker, *Phys. Rev.* **149**, 693 (1966).

<sup>3</sup> M. Ikeya, N. Itoh, and T. Suita, *J. Phys. Soc. Japan* **23**, 455 (1967).

<sup>4</sup> J. S. Nadeau, *J. Appl. Phys.* **34**, 2248 (1963); **35**, 1248 (1964).

<sup>5</sup> W. A. Sibley and E. Sonder, *J. Appl. Phys.* **34**, 2366 (1963).

<sup>6</sup> H. Rabin, *Phys. Rev.* **116**, 1381 (1959).

<sup>7</sup> H. Peisl, R. Balzer, and W. Waidelich, *Phys. Rev. Letters* **17**, 1129 (1966).

<sup>8</sup> G. J. Crowe, W. Fuchs, and D. A. Wiegand [*Phys. Rev. Letters* **16**, 1154 (1966)] interpret their results in terms of both Frenkel and Schottky damage.

<sup>9</sup> F. Seitz, *Rev. Mod. Phys.* **26**, 7 (1954).

<sup>10</sup> D. Pooley, *Solid State Commun.* **3**, 241 (1965); *Proc. Phys. Soc. (London)* **87**, 245 (1966); **87**, 257 (1966).

<sup>11</sup> H. N. Hersh, *Phys. Rev.* **148**, 928 (1966); J. D. Konitzer and H. N. Hersh, *J. Phys. Chem. Solids* **27**, 771 (1966).

<sup>12</sup> C. T. Bauer and R. B. Gordon, *Phys. Rev.* **126**, 73 (1962).

<sup>13</sup> J. D. Comins and P. T. Wedepohl, *Solid State Commun.* **4**, 537 (1966).

<sup>14</sup> P. V. Mitchell, D. A. Wiegand, and R. Smoluchowski, *Phys. Rev.* **121**, 484 (1961).

<sup>15</sup> W. A. Sibley and E. Sonder, *Phys. Rev.* **128**, 540 (1962).

<sup>16</sup> E. Sonder, W. A. Sibley, J. E. Rowe, and C. M. Nelson, *Phys. Rev.* **153**, 1000 (1967).

<sup>17</sup> W. A. Sibley, E. Sonder, and C. T. Butler, *Phys. Rev.* **136**, A537 (1964).

<sup>18</sup> J. H. Schulman and J. W. Boag, *Phys. Status Solidi*, **3**, 516 (1963).

<sup>19</sup> D. M. J. Compton, in *Proceedings of the International Symposium on Color Centers in Alkali Halides*, Urbana, Illinois, 1965, Abstract #31 (unpublished); Air Force Cambridge Research Laboratories Report No. 66-427, 1966 (unpublished).

<sup>20</sup> H. Rüchardt, *Z. Physik* **140**, 574 (1955); *Phys. Rev.* **103**, 873 (1956).

<sup>21</sup> B. Fritz, *J. Phys. Chem. Solids* **23**, 375 (1962).

<sup>22</sup> N. Itoh, B. S. H. Royce, and R. Smoluchowski, *Phys. Rev.* **137**, A1010 (1965); **138**, A1766 (1965).

<sup>23</sup> T. J. Neubert and J. A. Reffner, *J. Chem. Phys.* **36**, 2780 (1962).

<sup>24</sup> R. B. Murray and F. J. Keller, *Phys. Rev.* **150**, 670 (1966).

<sup>25</sup> H. Rabin, *Phys. Rev.* **129**, 129 (1963).

center concentration in KCl in the vicinity of room temperature.

### EXPERIMENTAL

In order to observe actual saturation of defects produced at room temperature rather than the apparent saturation of the extrinsic (impurity determined) first stage, long periods of irradiation at rather high dose rates were necessary. Therefore, we used a  $^{60}\text{Co}$   $\gamma$ -ray source which was ideal for such a study since its use did not require an operator and its intensity did not fluctuate, as would that of an x-ray machine or electron accelerator. In calculating the energy absorbed by the samples, we took into consideration the change in dose rate due to decay of the source. These measurements were performed during one and one-half years; thus the dose rate differed by approximately  $\pm 10\%$  from average value of  $1.85 \times 10^6$  R/h. Typically, three to four weeks of irradiation were necessary for each sample before saturation was approached; during that time, heights of color-center bands were measured every few days.

We quickly found that the saturation defect concentration was strongly dependent upon the temperature of the sample *during irradiation*.<sup>5</sup> Consequently, temperature control equipment was installed which permitted long-time control of the sample temperature to within  $0.2^\circ\text{C}$  during irradiation. Figure 1 is a schematic diagram of a typical controlled-temperature sample irradiation facility. The sensor is an immersion thermocouple, the calibration of which is not affected by  $\gamma$  irradiation. The actual sample temperature was determined periodically with a calibrated thermocouple inserted into the sample holder. The range of operation of these facilities is from the freezing point of the cooling water to about  $60^\circ\text{C}$ ; however, condensation of atmospheric moisture on the sample limited irradiations to temperature above  $10^\circ\text{C}$ . We found that warming samples from  $10^\circ\text{C}$  to room temperature of  $22^\circ\text{C}$  *in the absence of ionizing radiation* had no effect on the defect concentration. Thus, no error was introduced by bringing the samples to room temperature for measurement as long as they were returned to the experimental temperature before reinsertion into the source.

The  $F$ -center concentration, determined from the height of the  $F$  band at room temperature, was used as a measure of the total number of vacancies.<sup>26</sup> The height of the  $F$  band was either measured directly or was determined by curve fitting to better than 5% in

<sup>26</sup> The total number of vacancies includes  $F$ -aggregate centers, and is approximately 25% greater than the  $F$ -center concentration obtained from the  $F$  band. Also, it should be pointed out that a part of the  $F$ -aggregate center absorption appears under the  $F$  band [F. Okamoto, Phys. Rev. 124, 1090 (1961)]. We attempted to analyze the kinetic behavior of only  $F$  centers, obtained by subtracting the aggregate center contribution from the  $F$ -band absorption as well as the total vacancy concentration, as obtained from the sum of the  $F$  band and  $F$ -aggregate band areas. Neither of these more laborious approaches yielded results essentially different from those described herein.

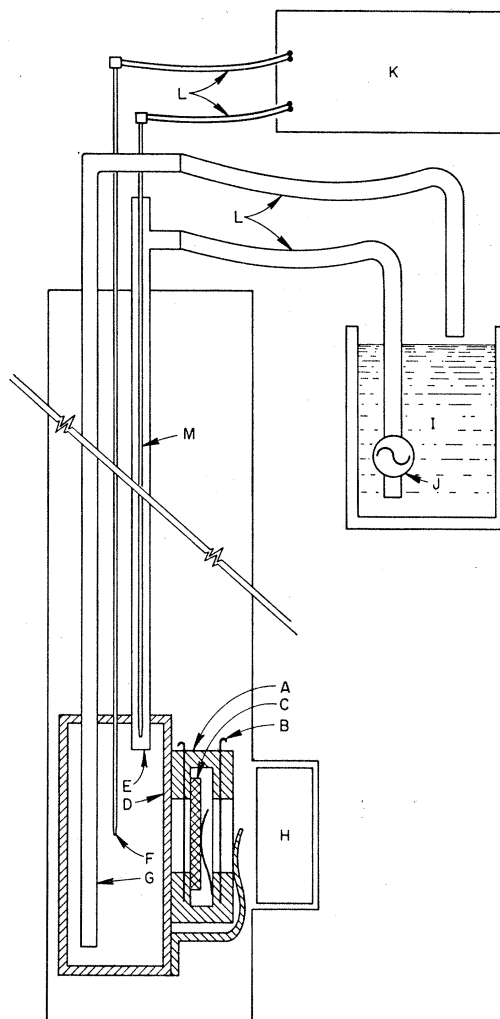


FIG. 1. Diagram of temperature-controlled sample irradiation facility. A, removable sample holder that also fits into spectrophotometer. B, sample holder slides to permit keeping the sample (C) in the dark at all times except when spectra are being measured. D, water-filled constant-temperature chamber with water input tube (E), immersion thermocouple (F), and water exhaust tube (G). H,  $^{60}\text{Co}$  source located 8 ft below ground level. I, Refrigerated water bath and pump (J). K, temperature controller made up of ice reference junction, reference voltage source, and magnetic amplifier controller with rate action, Series 1000, Electronic Control Systems, Inc. L, Flexible hoses and leads to make possible raising of the constant-temperature facility from the vicinity of the  $\gamma$  source to ground level. M, Immersion heater, Conax  $\frac{1}{8}$ -in.-diam, inserted in water supply tube.

cases where the optical density at the  $F$ -band peak was greater than could conveniently be measured with the Cary 14R spectrophotometer (o.d.  $\sim 5$ ).

In order to assess whether the saturation of  $F$ -center growth was indeed due to an equilibrium between production and annihilation reactions, it was necessary to discover if the same saturation concentrations could be approached by annihilating an excess of defects, as could be reached by production. This was accomplished

by making use of the intensity dependence<sup>27</sup> or the temperature dependence of the production and annihilation processes. By using an electron accelerator, a much higher energy deposition rate,  $5 \times 10^{12}$  MeV/sec  $\text{cm}^3$  as compared to  $6 \times 10^{10}$  MeV/sec  $\text{cm}^3$  for the  $\gamma$  source, could be achieved. This made it possible to attain an  $F$ -center concentration in excess of the saturation concentration that could be produced with the  $\gamma$  source. Inserting a sample thus preirradiated into the normal sample position of our  $\gamma$  source permitted the observation of radiation-induced annihilation of defects. Similarly, preirradiating a sample at a lower temperature produced an excess defect concentration whose decay could be observed by subsequent irradiation at a higher temperature.

## RESULTS

### Defect Saturation

In Fig. 2 is shown a typical set of data obtained from alternate irradiations and  $F$ -band absorption measurements. We have labeled regions I-V and have drawn inserts to facilitate this description. Regions I and V depict the approach to saturation from below (lower concentrations) and above (higher concentrations) when the sample is irradiated with  $\gamma$  rays. In regions II-III an excess defect concentration has been produced by irradiation at a higher dose rate, using the electron accelerator. The apparently discontinuous jumps, labeled II and IV, which are shown expanded in the inserts, reflect changes in the vacancy aggregation ( $F$  center- $M$  center) equilibrium that have been re-

ported previously.<sup>27-30</sup> In region II this equilibrium shifts to favor  $F$  centers at the expense of  $M$  and other aggregate centers. Conversely, in region IV the aggregation equilibrium appropriate for the lower dose rate is reestablished. We will say little more about this aggregation since we are concerned here with the processes connected with defect production and annihilation, which, as can be seen from Fig. 2, are about two orders of magnitude slower than the processes leading to the aggregation steady state. Needless to say, on the time scale of our figures (with the exception of the expanded inserts) the aggregation steady-state condition exists at all times. This is confirmed by our measurements where (again with the exception of times immediately after changing of intensity or temperature as in regions II and IV) every increase or decrease in  $F$ -center concentration is accompanied by a corresponding increase or decrease in the concentration of aggregate centers.

A series of growth and decay curves for samples from two different crystals are depicted in Figs. 3(a) and 3(b). The different curves are for samples whose temperatures differed during irradiation. Excess defect concentrations in this figure were produced by irradiating at higher dose rates. Clearly the saturation levels attained from above are the same as those approached from below for the same conditions.

In Fig. 4 are shown results of an experiment in which the excess defect concentration was obtained by irradiation at a lower temperature. In this experiment the temperatures of two samples were interchanged. The results are similar to those depicted in Fig. 3 :

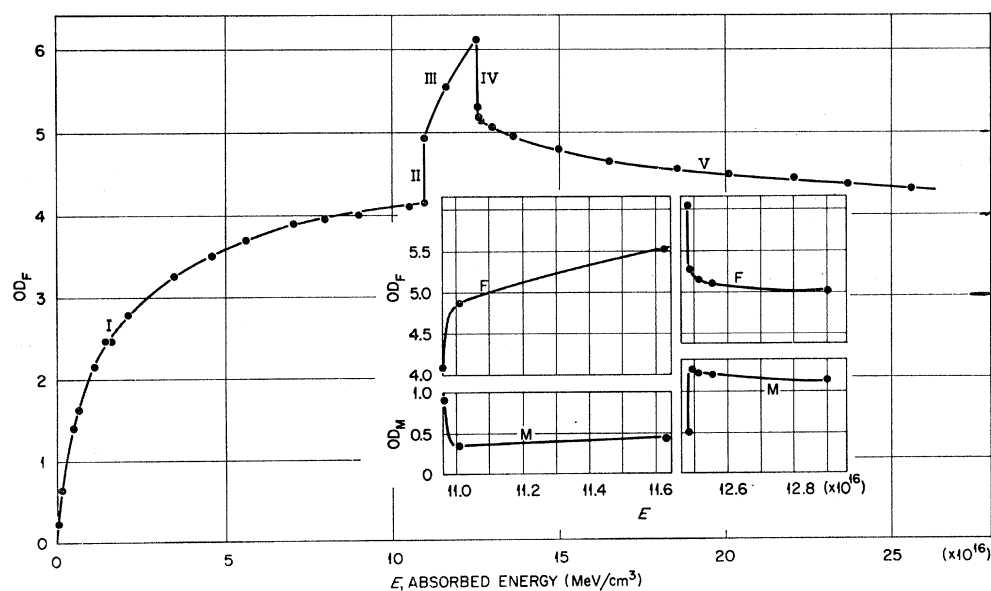


FIG. 2. Typical  $F$ -center saturation curve for KCl being  $\gamma$  irradiated at  $19.9^\circ\text{C}$  at a dose rate of  $6 \times 10^{10}$  MeV/sec  $\text{cm}^3$  (regions I, IV, and V) and  $5 \times 10^{12}$  MeV/sec  $\text{cm}^3$  (regions II and III). In the inserts of  $F$ - and  $M$ -center optical density is reproduced on an expanded time scale for the rapidly changing portions of the curve obtained after changing the dose rate (regions II and IV).

<sup>27</sup> E. Sonder and W. A. Sibley, Phys. Rev. **129**, 1578 (1963).

<sup>28</sup> P. G. Harrison, Phys. Rev. **131**, 2505 (1963).

<sup>29</sup> S. Schnatterly and W. D. Compton, Phys. Rev. **135**, A227 (1964).

<sup>30</sup> H. G. Dahnke and K. Thommen, Z. Physik **184**, 367 (1965).

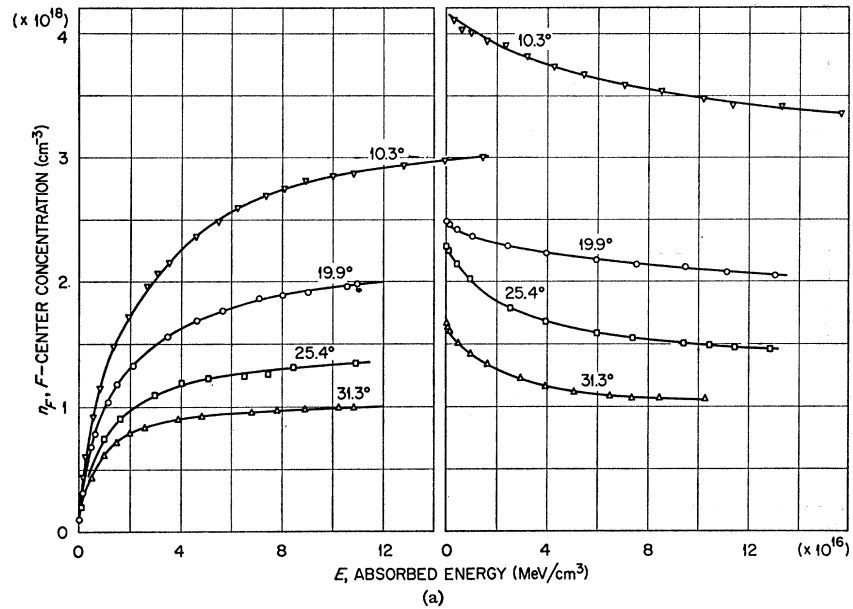
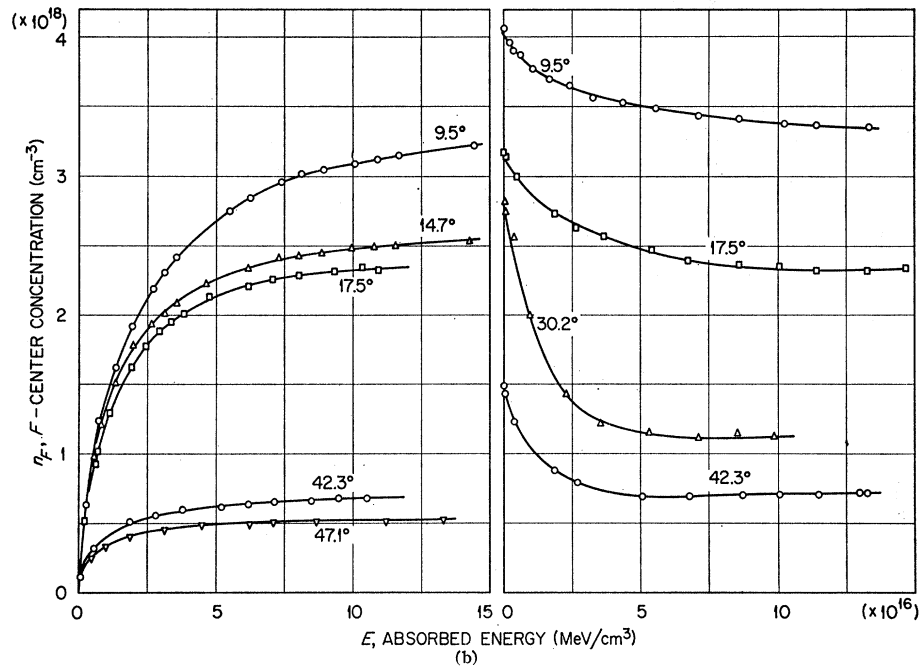


FIG. 3. Saturation behavior of  $F$  centers produced by  $\gamma$  irradiation. Figure 3(a) is for samples from crystal H410 purchased from Harshaw. Figure 3(b) is for samples from crystal 1223 grown at Oak Ridge National Laboratory. The left half of the curves depicts the approach to saturation during  $F$ -center growth at a dose rate of  $6 \times 10^{10}$  MeV/cm<sup>3</sup> sec at temperatures given on the figures in °C. The right half depicts the decay of an excess  $F$ -center concentration produced by preirradiation at a higher dose rate.



The saturation level is the same whether attained from below or above.

It is evident from Figs. 3 and 4 that the defect concentration attained after long irradiation of nominally pure KCl is a function principally of the dose rate used and of the radiation temperature. It might also be expected to depend on trace impurities.<sup>17</sup> However, since the same results are obtained for a sample grown at this laboratory [Fig. 3(b)] and one purchased from Harshaw [Fig. 3(a)] and since, as shown in Table I, these samples contain different amounts of trace impurities, it follows that for the dose rate used the

impurities indicated in Table I have little effect upon the defect saturation level. It should be pointed out that as little as  $\frac{1}{2}$ –1 ppm lead or silver will depress the saturation level and that large amounts of impurities will, as has been shown previously,<sup>17</sup> suppress late-stage coloration almost completely.

The temperature dependence of the saturation level can be plotted semilogarithmically as shown in Fig. 5 to yield an apparent activation energy of 0.4 eV. This is an empirical value and should not be taken blindly as an activation energy for any particular process.

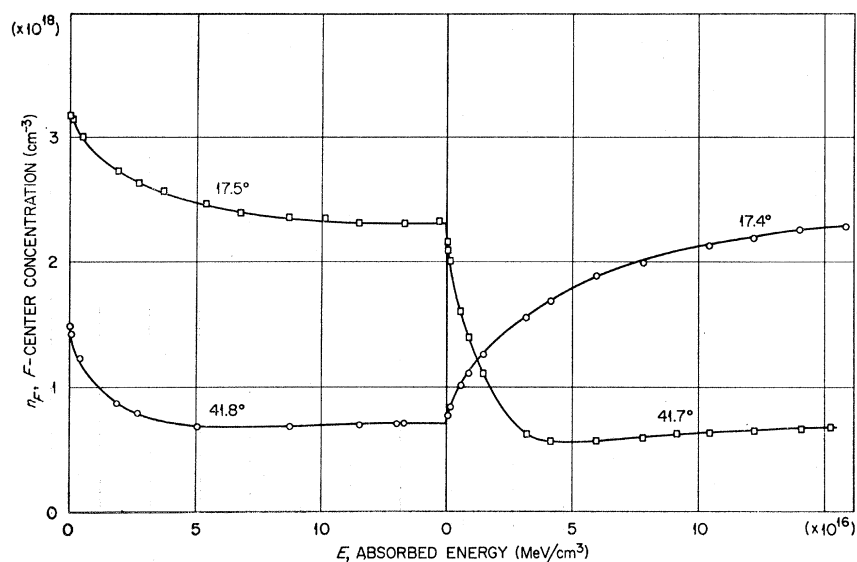


FIG. 4. Change in saturation level upon changing irradiation temperature. The curves show the growth and decay of the  $F$ -center concentration when the temperatures at which two samples are irradiated are changed. Temperatures are given in  $^{\circ}\text{C}$ .

#### Approach to Saturation

In Fig. 6 is shown the approach to saturation from below and from above on a semilogarithmic scale for a number of temperatures. If the equilibrium were simply the result of a constant rate of production of defects  $A$  and of a rate of annihilation  $Bn$  which is

$$dn/dt = A - Bn \quad (1)$$

would be as suitable description. The solution of Eq. (1),  $n = A/B[1 - \exp(-Bt)]$  would yield straight lines in Fig. 6. Moreover, this description would predict that the slope  $B$  be independent of whether saturation is approached from above or below. Clearly the curves are not straight lines; nor is there any similarity between corresponding approach curves from above and below. It might be argued that deviation of the curves from straight lines might be due to aggregation side reactions. However, plotting the data using the total concentration (including aggregate centers) of negative-ion vacancies, still resulted in curves similar to those shown in Fig. 6, and not in straight lines.

In analyses of approach to saturation it is often the practice when a single exponential function does not suffice to attempt to fit a sum of exponential functions. Almost any saturating curve can be fitted in this manner; our curves yielded to such analysis using two exponentials. However, no consistent trend appeared in the parameters, indicating that such treatment was

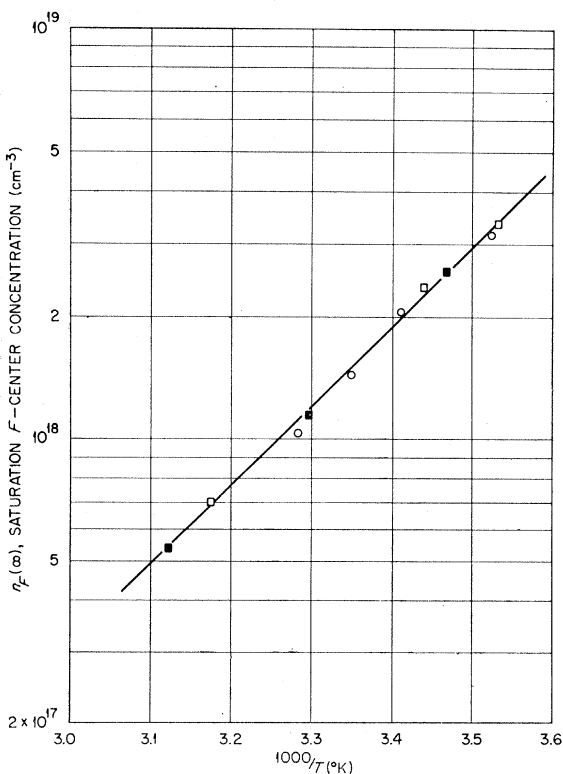


FIG. 5. Semilogarithmic plot of saturation  $F$ -center concentration versus reciprocal temperature. The circles are for the crystal H410; the squares are for samples from crystal 1223.

TABLE I. Impurities in KCl samples.

Crystal designation	Impurity $\mu\text{g/g}$ (KCl)					Net polyvalent <sup>e</sup> positive ions (ppm)	
	Br <sup>a</sup>	I <sup>b</sup>	Na <sup>c</sup>	Rb <sup>c</sup>	OH <sup>d</sup>	Pb <sup>d</sup>	
H410	95	<1	3	7	0.01	<0.01	0.08
1223	0.9	<1	6	19	0.001	<0.01	0.5

- <sup>a</sup> Activation analysis.  
<sup>b</sup> Wet chemistry.  
<sup>c</sup> Flame photometry.  
<sup>d</sup> Optical absorption.  
<sup>e</sup> Ionic conductivity.

not significant. In particular, the slopes for long times in Fig. 6, which should reflect the temperature dependence of the saturation levels, do not do so.<sup>31</sup> We concluded therefore that a simple rate equation of the form given [Eq. (1)] was not adequate. Moreover, a generalization of Eq. (1) whose solution would yield two exponentials which would imply that two simultaneous annihilation processes are operating, was unsatisfactory. It appears that factors other than the temperature and dose rate (the determining factors for the saturation level itself) influence the details of the approach to saturation.

A hint to the identity of these factors is contained in Fig. 4 in the rapid decay of  $F$  centers apparent in the curve for the sample raised from 17.5 to 41.7°C. A careful look at that decay curve will reveal that the  $F$ -center concentration passes through a minimum, after which it approaches the saturation level from below. This behavior suggests that previous history, in particular the temperature during previous irradiation, influences subsequent growth and decay of the vacancy concentration.

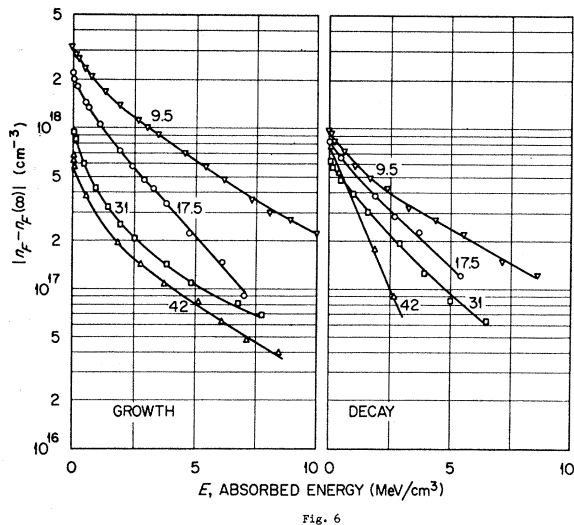


FIG. 6. Approach curves plotted to compare with a solution to Eq. (1). The ordinate of the curves on the left is the  $\log[n_F(\infty) - n_F]$ ; that of the curves on the right is  $\log[n_F - n_F(\infty)]$ , where  $n_F$  is the  $F$ -center concentration produced by the absorbed energy given on the abscissa scale, and where  $n_F(\infty)$  is the saturation  $F$ -center concentration. Radiation temperatures are given on each curve in °C.

<sup>31</sup> From the solution of the simple rate equation it is clear that if  $A$  and  $B$  are temperature activated,  $A = A_0 \exp(-E_A/kT)$ ,  $B = B_0 \exp(-E_B/kT)$ , then the saturation level,  $n(t = \infty) = A/B$ , is fixed by an energy parameter  $E_B - E_A$ , analogous to a chemical reaction energy, while the slope of the exponential approach curves of the type plotted in Fig. 6 exhibits an activation energy  $E_B$ . Since  $E_A$  cannot be negative, the slope of approach curves has to have a stronger temperature dependence than the saturation level. Similar reasoning can be applied to the long-time limiting slope in a treatment in which a number of exponential terms are treated, i.e.,  $dn/dt = A - \sum B_i n_i$  where  $n = \sum n_i$ .

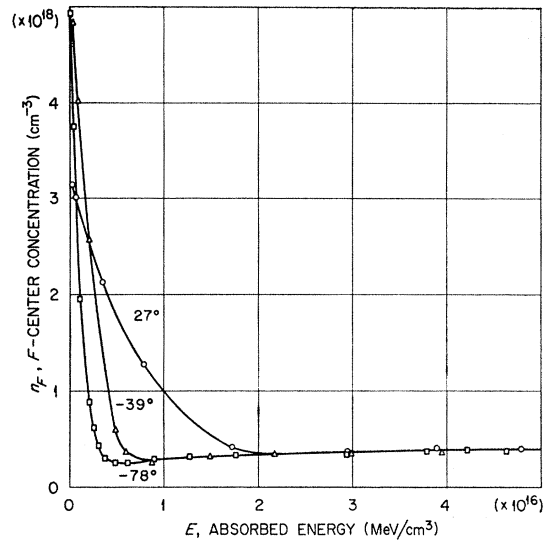


Fig. 7. Decay of  $F$  centers produced by preirradiating at different temperatures. The decay is produced by irradiating at 47°C in a  $\gamma$  source. The temperatures given on the curves refer to the temperature in °C during preirradiation with an electron accelerator.

### Effect of Previous Temperature

In order to confirm this surprising observation, we preirradiated three samples with the electron accelerator. Conditions were identical except for the temperatures; these were  $-78$ ,  $-39$ , and  $27^\circ\text{C}$  obtained by using dry ice, Freon 22, and air for cooling. Subsequent  $\gamma$  irradiation at  $47^\circ\text{C}$  (for all three samples) resulted in the curves shown in Fig. 7. Just as for the sample shown in Fig. 4, the  $F$ -center concentrations go through a minimum. The decay is clearly much slower for the sample preirradiated at room temperature than for the samples that had been irradiated at lower temperature. This effect is not related to the  $F$ -center concentration, since the  $F$ -center concentrations after preirradiation were 5, 6, and  $3 \times 10^{18} \text{ cm}^{-3}$  (i.e., not monotonic) for  $-78$ ,  $-39$ , and  $27^\circ\text{C}$ , whereas, the decrease of the decay rate was monotonic with radiation temperature. As was the case for the other samples, the decay and approach to the base curve were not simply exponential in time.

### CONCLUSION AND DISCUSSION

We can summarize the experimental results by the following three statements:

1. After long irradiation in the vicinity of room temperature, the color-center concentration in KCl saturates at a level that depends upon dose rate and temperature. The temperature dependence in undoped material can be described by an activation energy of 0.4 eV between 10 and  $50^\circ\text{C}$ .
2. The approach to saturation cannot be described

by a single exponential approach function. Moreover, there is no apparent relation between the temperature dependence of the approach rate and that of the saturation  $F$ -center concentration.

3. The decay rate and approach to equilibrium after preirradiation are strongly dependent upon the temperature during preirradiation.

Even though these results cannot be described by a simple rate equation, statement 1 nevertheless requires that a process for annihilation of  $F$  centers exists during irradiation, in addition to a process for production of  $F$  centers. This is not too surprising since we now are aware of the fact that one of the forms of the negative-ion vacancy (the  $\alpha$  center according to Lüty<sup>32</sup>) is mobile during bleaching and irradiation, permitting  $F_A$ <sup>33</sup> and  $F$ -aggregate center formation. This mobile vacancy would be expected to recombine with its anti-center during irradiation, causing defect annihilation.

Although these data in themselves can be accounted for in other ways, we shall examine them in terms of a diffusion-limited annihilation reaction between mobile vacancies and interstitial clusters acting as sinks. The rate law for such a process has been derived.<sup>34</sup> Using such a rate law, Eq. (1) can be replaced by

$$dn_F/dt = A - 4\pi rNDn_V, \quad (2)$$

where  $r$  is the radius of an average interstitial cluster,  $D$  is the diffusion coefficient of the mobile vacancy,  $N$  is the interstitial cluster (sink) concentration, and  $n_V$  is the concentration of negative-ion vacancies. Equation (2) is not soluble without a great deal more information than we have now; there are really three relations involved since  $n_F$ ,  $n_V$ ,  $N$ , and  $t$  are all variables. The difficulty lies in relating the variables  $N$  and  $n_V$  of this equation to the  $F$ -center behavior of the data. The mobile vacancy concentration  $n_V$  may be proportional to  $n_F$  but probably varies with it more slowly than linearly and probably depends also upon the radiation dose rate and the concentration of electron trapping trace impurities. The sink concentration can be written as  $N = n_F/\alpha$ , where  $\alpha$  represents the average number of interstitials per cluster.  $\alpha$  probably increases slowly as the  $F$ -center concentration increases. Thus, the annihilation term of Eq. (2) which would vary as fast as  $n_F^2$ , if both  $n_V$  and  $N$  were strictly proportional to  $n_F$ , probably varies much more slowly, suggesting that a second-order rate equation of the form  $(dn/dt)A' - B'n^2$  is no better description than is a first-order equation. In this connection we have attempted to fit some of the data of Fig. 6 to a second-order rate equation; the fit was even poorer than it was to Eq. (1).

<sup>32</sup> F. Lüty, in *Physics of Color Centers*, edited by W. Beall Fowler (Academic Press Inc., New York, to be published), Chap. 3.

<sup>33</sup> H. Härtel and F. Lüty, *Z. Physik* **177**, 369 (1964); **182**, 111 (1964).

<sup>34</sup> See, for instance, A. C. Damask and G. J. Dienes, *Point Defects in Metals* (Gordon and Breach, Science Publishers, Inc., New York), 1963, Ch. 2.

The preirradiation effect (conclusion 3) can be accounted for in a rather straightforward fashion within this framework. Previously reported experimental work<sup>16</sup> suggests that the defect structure, in particular the size of the interstitial cluster produced by radiation, depends upon the temperature during radiation, and is larger for higher radiation temperatures. It is fairly easy to reason from this that for the case of a sample that has been preirradiated at a low temperature the parameter  $\alpha$  is small initially, yielding a large annihilation rate. The lower the preirradiation temperature is the smaller will be  $\alpha$  and the faster will be the initial annihilation rate. Eventually the average cluster size approaches that appropriate for the conditions of the final irradiation and the decay term decreases enough to permit approaching the saturation level from below. The fact that the cluster size  $\alpha$  is a function of the condition under which previous irradiation has occurred also accounts for the different shape of corresponding production and decay curves in Fig. 6.

The experimentally determined reaction energy of 0.4 eV, contains not only the diffusion energy, which according to Lüty is 0.6 eV, but contains also any exponential temperature dependences that may be present in the production term  $A$ , in the constant relating  $n_V$  to the  $F$ -center concentration  $n_F$ , and in the long-time limiting cluster size  $\alpha$  ( $t = \infty$ ).

Although as the above discussion shows it is not possible to evaluate any parameters by fitting the results to a rate equation, we can make an estimate of the parameter  $\alpha$  by comparing the characteristic approach time for two processes; the  $F$ -center interstitial cluster annihilation, and the  $F$ -aggregation reaction which determines the rate of  $M$ -center growth when the temperature or dose rate is changed. On the assumption that these two reactions are both controlled by diffusion of the negative-ion vacancy, we can write, for instance, for the initial  $M$ -center production (aggregation) rate in region IV of Fig. 2,

$$dn_M/dt|_{t=0} = 4\pi r_0 n_F' D n_V, \quad (3)$$

where  $r_0$  is the trapping radius of an  $F$  center for a mobile vacancy to form an  $M$  center. The initial approach rate to  $F$ -center saturation is, according to Eq. (2)  $A$ , but if we assume  $A$  to be dependent only upon external conditions, then at long times (saturation)  $A = 4\pi rNDn_V$ , so that the ratio

$$\frac{|dn_M/dt|_{t=0}}{|dn_F/dt|_{t=0}} = \frac{4\pi r_0 n_F' D n_V}{4\pi rNDn_V} = \frac{3r_0}{2r} \alpha. \quad (4)$$

The factor  $\frac{3}{2}$  is included since  $n_F'$  (region IV, Fig. 2)  $\simeq \frac{3}{2}n_F = \frac{3}{2}\alpha N$ . There are two assumptions we can make about  $r$  and  $r_0$ : We can assume that either the interaction radii of  $F$  centers and interstitial clusters are comparable, in which case the ratio of approach rates yields  $\alpha$ , or the sink volumes are geometric, in which case  $4\pi r^3 \simeq 4\pi r_0^3 \alpha$  or  $r/r_0 \simeq \alpha^{1/3}$ . The latter assumption

TABLE II. Interstitial cluster size.

F-Center decay rate at 30°C (centers/MeV sec)		Ratio of rates	Number of interstitials per cluster	
During aggregation	During annihilation		Assume equal cross section	Assume geometric cross section
$(9 \pm 1) \times 10^8$	$(2 \pm \frac{1}{2}) \times 10^8$	$\sim 50$	$\sim 35$	$\sim 200$

appears to be more reasonable. Table II gives the values for the size of the interstitial clusters for irradiation in the vicinity of room temperature obtained using these assumptions. Clearly even for comparable inter-action radii the results imply rather large clusters.<sup>35</sup>

<sup>35</sup> These estimates are based on the assumption that random diffusion controls both the annihilation and aggregation of nega-

## ACKNOWLEDGMENTS

The authors would like to thank other members of the insulator group in the Solid State Division of ORNL, particularly W. A. Sibley, for very helpful discussions of the results. We thank J. R. Russell, C. T. Butler, and B. Quincy of the Research Materials group for providing one of the crystals used for this study. Members of the Analytical Chemistry Division performed numerous chemical analyses, from which we were able to appraise the trace impurity content of our samples.

tive-ion vacancies. If M-center formation were due, for example, to highly correlated combination of nearby *F* centers [see, e.g., Y. Farge, M. Lambert, and R. Smoluchowski, *Solid State Commun.* 4, 333 (1966)], then the above comparison would be invalid.

## Interaction Potentials of Gas Atoms with Cubic Lattices on the 6-12 Pairwise Model

FRANK O. GOODMAN

*Daily Telegraph Theoretical Department, School of Physics, University of Sydney,  
Sydney, New South Wales, Australia*

(Received 26 June 1967)

The interaction potential energy of a gas atom with a solid is obtained by summing the 6-12 gas-atom-solid-atom pairwise potential over all atoms of a perfect, monatomic, cubic, semi-infinite lattice model. Study is made of relations among (i) heats of adsorption, surface diffusion, and sublimation; (ii) lattice spacing, lattice type [body-centered and face-centered cubic], and exposed lattice face [(100) and (110)]; and (iii) the pairwise interaction parameters. Possibilities of obtaining one or more of these quantities from knowledge of the others are considered. The theory is applied to an analysis of experimental data, and a somewhat unsuccessful attempt is made to assess the validity of the 6-12 pairwise model in gas-surface interactions. Tables, correct to five significant figures, of sums of inverse sixth and twelfth powers of gas-atom-solid-atom distances are presented as functions of distance of the gas atom from the surface of a simple cubic lattice which has either its (100) or its (110) face exposed.

## I. INTRODUCTION

EXAMINATION is made of the assumption that the interaction of a gas atom with a solid may be described by means of a potential energy obtained by a summation over all atoms of the solid of the Lennard-Jones 6-12 gas-atom-solid-atom pairwise interaction potential<sup>1</sup>:

$$V_{ij}/\epsilon = (r_0/r_{ij})^{12} - 2(r_0/r_{ij})^6. \quad (1)$$

$V_{ij}$  is the potential energy of interaction of atoms  $i$  and  $j$  separated by a distance  $r_{ij}$ ;  $r_0$  and  $\epsilon$  are the 6-12 gas-atom-solid-atom parameters, the physical significance of which is well known. The solid is represented by a perfect, monatomic, cubic, semi-infinite lattice model, and the interaction potential of a gas atom near the surface is assumed to be obtained by summing (1)

over all atoms  $j$  of the semi-infinite lattice with  $i$ = gas atom.

The lattice type is denoted by L, and a notation of Born<sup>2</sup> is used: L=s, b, and f denote, respectively, the simple, body-centered and face-centered cubic lattices. The lattice spacing is  $a$  (the nearest-neighbor distances are  $q^{1/2}a/2$ , where  $q=4, 3$ , and  $2$ , respectively, for s, b, and f lattices). The exposed face F of the lattice must be specified [F=(110), for example] and the notation used is that FL means the F face of the L lattice; the conventional round brackets in the face specification are omitted hereafter (for example, F=110).

Questions to which we attempt partial answers are the following:

(1) What is the atomic heat  $H$  of adsorption at zero coverage and the corresponding "heat" (activation

<sup>1</sup> J. E. Lennard-Jones, *Physica* 4, 941 (1937).

<sup>2</sup> M. Born, *Proc. Cambridge Phil. Soc.* 36, 160 (1940).